Two-photon absorption cross-sections and time-resolved fluorescence imaging using porphyrin photosensitisers†

Sean Mathai,[a] Damian K. Bird,[a] Stan S. Stylli,[b] Trevor A. Smith*[a] and Kenneth P. Ghiggino[a]

Received 3rd April 2007, Accepted 5th July 2007
First published as an Advance Article on the web 19th July 2007
DOI: 10.1039/b705101h

Three porphyrin systems have been characterised for use in two-photon fluorescence imaging of biological samples. We have determined the two-photon absorption cross sections (σ_2) of the di-cation, free-base and metallated forms of hematoporphyrin derivative (HpD), hematoporphyrin IX (Hp9) and a boronated protoporphyrin (BOPP) using the open-aperture Z-scan and the two-photon induced fluorescence (TPIF) techniques at an excitation wavelength of 800 nm. The insertion of either protons or a metal ion into the macrocycle is shown not to significantly influence the σ_2 of the porphyrins. Two-photon time-resolved fluorescence images of C6 glioma cells transfected with a free-base form of the BOPP have been obtained as a function of the porphyrin concentration. These studies reveal a maximum useful porphyrin concentration for fluorescence imaging purposes of approximately 30 μg mL^{-1}.

Introduction

Molecules exhibiting nonlinear optical response are used in a variety of applications including all-optical switching,[1] ultrashort pulse characterisation,[2,3] optical power limiters[4,5] microfabrication[6,7] and three dimensional optical data storage.[8] An in depth treatment of the theory used to explain nonlinear processes may be found elsewhere.[9,10] The advent of ultrashort pulsed lasers has meant that nonlinear processes are now able to be investigated reasonably routinely. One such nonlinear process that has been receiving a great deal of interest is two-photon absorption. Two-photon absorption involves photons that are normally unable to induce an excitation event individually, being absorbed "simultaneously" by the molecule under investigation. The first photon provides sufficient energy to promote an electron to a virtual state,[11] which is considered to be a state with a sufficiently short lifetime such that it is described to have a completely undefined energy due to the uncertainty principle. The second photon interacts with the electron in the virtual state within the duration of the population of the virtual state, (approximately 10^{-18} s)[12] to induce excitation to a higher electronic excited state. Once excitation of the molecule is achieved, the subsequent relaxation processes are identical to those observed proceeding from a single-photon absorption event.[13,14]

Whilst numerous advantages of multi-photon excitation over single photon excitation are put forward, there are still many disadvantages. One of the often-stated key advantages of multi-photon excitation is the potentially increased penetration depth of the incident radiation, compared to single photon excitation, into biological material. The enhancement in penetration depth is achieved by exploiting the optical transmission window of biological tissue existing in the NIR region by the use of two-photon excitation. An enhanced image quality in light scattering, turbid media such as cells can also be achieved with a two-photon method of excitation due to the relationship between the scattering produced by the small particles within a cell being proportional to the inverse fourth power of the excitation wavelength.[15,16] Dispersion effects in condensed and highly scattering materials can reduce these advantages due to the strong dependence of two-photon absorption efficiency on excitation peak power. Two-photon fluorescence microscopy eliminates out of focus influences by confining the detected signal to the plane where the photon density is sufficiently large to allow two photons to interact simultaneously. This method offers many benefits over previously used techniques, such as confocal microscopy, including a marked reduction in the photobleaching and heating of the sample, of particular importance in biological applications.[12,16–18] However, the benefits achievable from a two-photon method of excitation are not limited to providing improvements in the image quality of biological tissue, with a great deal of interest currently being focused on investigating a two-photon induced method of photodynamic therapy[19–22] with the potential of providing an additional enhancement in the selectivity of the treatment of cancer cells as well as facilitating the treatment of deeper lying tumours.

The extremely short lived virtual intermediate state involved in facilitating a two-photon absorption event accounts for the diminutive nature of the two-photon absorption cross sections (σ_2) routinely observed.[13] Organic compounds are known to exhibit small nonlinearities, yet a significant amount of interest has been shown in investigating such materials, largely due to their good mechanical, chemical, thermal and optical stability. One such class of organic compounds is the tetrapyrrolic compounds (porphyrins, chlorins, bacteriochlorins). These compounds also provide excellent templates for the "tailoring" of the structures by the addition of central metal ions or peripheral substituents.[23]

[a]*School of Chemistry, The University of Melbourne, Victoria, 3010, Australia. E-mail: trevoras@unimelb.edu.au; Fax: +61-3-9347 5180; Tel: +61-3 8344 6272*
[b]*Department of Surgery, Royal Melbourne Hospital, Parkville, 3052, Australia*
† This paper was published as part of the special issue in honour of David Phillips.

Additionally, the highly developed π-electron conjugation system characteristic of porphyrins makes them attractive candidates for exhibiting a large nonlinear response.[24,25]

Two major techniques are used to characterise the two-photon absorption properties of a molecule. The Z-scan technique provides an easy and direct method for determining both the real and imaginary parts of the third-order nonlinear susceptibility $\chi^{(3)}$ in solids, liquids and liquid solutions.[26,27] The imaginary and the real parts of $\chi^{(3)}$ relate to the two-photon absorption (TPA) and nonlinear refractive index, respectively.[10] The experiment involves monitoring the change in transmission as a sample is translated through the focal point of a focussed laser beam. The laser beam is attenuated as the light intensity becomes sufficiently high to induce higher order optical effects. The resultant change in transmission is recorded by a photon detecting device placed in the far field. The real part of the third order nonlinear susceptibility is determined by placing an aperture in front of the detecting device, named a closed aperture Z-scan. Nonlinear absorption can be determined directly by removing the aperture in an open aperture Z-scan. The nature of the experiment necessitates the use of high concentration samples in order to record observable changes in the attenuation of the beam as the sample is moved through the focal area.

The TPIF technique encompasses several advantages over the transmission based Z-scan technique. The detection of the fluorescence intensity rather than monitoring the slight changes in the attenuation of the beam results in the ability to use excitation intensities that are up to ten times lower and sample concentrations three orders of magnitude lower than those needed for the transmission based experiments.[28] The use of lower intensities allows contributions from higher order nonlinearities that interfere with the determination of σ_2 to be minimised and the use of lower concentration samples, limits photophysical changes of the sample arising from dimer or higher aggregate formation.

We have determined the σ_2 of different forms of three porphyrins using both the transmission based open aperture Z-scan and the emission-based two-photon induced fluorescence experiments. The values obtained provide a means of establishing the potential for using these compounds in two-photon induced photosensitisation and as fluorophores in two-photon time-resolved microscopy. Successful two-photon time-resolved fluorescence microscopy of a boronated porphyrin in a tumour cell line is reported, and provides insight into the different micro-environments found within the various regions of the cell.

Materials and methods

Chemicals

Hematoporphyrin IX dihydrochloride (Hp9, Porphyrin Products), hematoporphyrin derivative (HpD, Porphyrin Products), the tetrakiscarborane carboxylate ester of 2,4-(α,β-dihydroxyethyl)deuteroporphyrin IX (BOPP, synthesised as described previously[29] and provided by S. Stylli, Royal Melbourne Hospital), Rhodamine 6G (Rh6G, Aldrich), Rhodamine B (RhB, Lambda Physik) and Fluorescein (F, BDH Chemicals) were all used as received. The organic solvents methanol (ICN Biomedicals Inc.), ethanol (Merck) and acetone (Ajax Fine Chemicals) were of spectroscopic grade and used as supplied. The chemical structures of these porphyrins are given in Fig. 1. Note that HpD is known

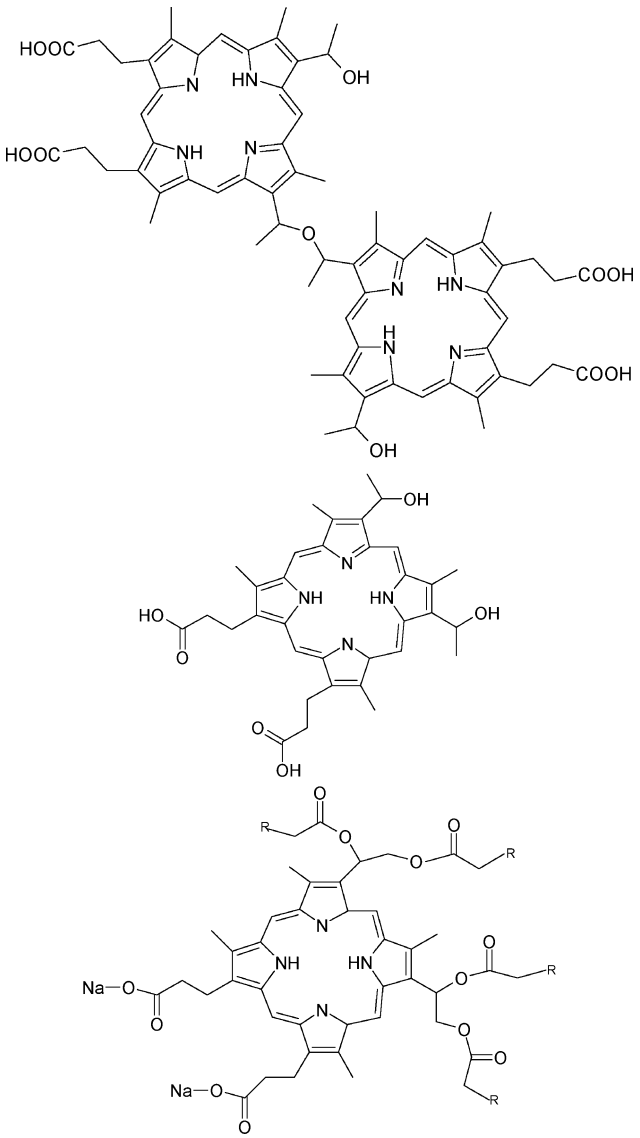

Fig. 1 Chemical structures of the porphyrins studied (a) HpD, (b) Hp9 and (c) BOPP (R = *closo*-1,2-$B_{10}C_2H_{11}$ pendant cages).

to consist of a mixture of oligomers and dimers, and the structure given is the dimeric representation.

The di-cation forms of the porphyrins were prepared by the addition of aqueous hydrochloric acid to achieve the desired pH, monitored with a pH meter (Cyberscan 1000 Activon). Zinc complexes of the porphyrins were prepared by the addition of a few drops of concentrated aqueous zinc(II) sulfate ($ZnSO_4$, BDH) solution to the free-base porphyrin samples. These were allowed to stand in the dark for approximately 72 h. The coordination of the metal was confirmed by observing a change in the acquired steady state absorption spectra associated with the altered symmetry assignment of the macrocycle.[30]

Steady-state experiments

Steady-state absorption measurements were recorded on a Varian Cary Bio50 UV-Vis absorption spectrophotometer. Absorption spectra were obtained prior and post irradiation to detect for any photodegradation of the samples. Steady state fluorescence

emission and excitation spectra were collected using a Cary Eclipse fluorescence spectrophotometer with excitation and emission bandwidths set to 5 nm. The samples were prepared to have an optical density at the excitation wavelength of approximately 0.1 in order to reduce inner-filter effects. All fluorescence excitation and emission spectra were collected from un-degassed samples contained in a 1 cm pathlength quartz cell.

Open-aperture Z-scan experiment

Fig. 2 shows the open aperture Z-scan experimental setup. An 18 W CW Nd:Vanadate laser (Coherent Verdi V18) is used to pump a Ti:Sapphire oscillator (Coherent, Mira 900F) operating at 76 MHz with pulse duration of approximately 90 fs (FWHM). The system is capable of producing pulses in the wavelength range of approximately 700–1000 nm. For all experiments in the current study, all laser systems were tuned to 800 nm. A 1 : 2 beamsplitter allowed the MIRA oscillator to be pumped by 6 W and a regenerative amplifier (REGA 9000, Coherent, ~200 fs duration at 250 kHz) to be pumped by the remaining 12 W from the V18 laser. The MIRA was used to seed the REGA in order to obtain higher energy pulses in the order of microjoules compared to the nanojoule pulses obtained from the output of the oscillator.

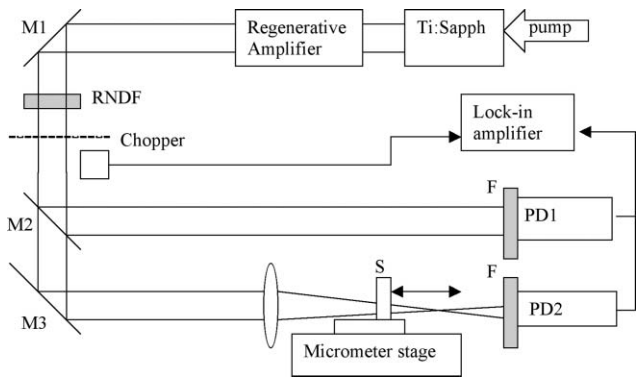

Fig. 2 Schematic of experimental setup for the open aperture Z-scan experiment: M1–M3: mirrors; S: sample; F: filters; RNDF: rotatable variable neutral density filter; PD1 and PD2 are the reference and sample photodiodes respectively.

The output from the REGA was passed through a continuously variable metallic neutral density filter (NDC-25C-2M, Thor labs). The neutral density filter allowed for variation of the incident energy with subsequent scans. The average power of the attenuated laser beam was measured using an optical power meter (Ophir Nova) with a high-power head (30A-SH-V1) before and after each scan. Laser average powers were measured at the position immediately prior to the sample to account for as much of the beam attenuation from the optics as possible. The incident beam was focussed using a 25 cm plano-convex lens (KXP 113, Newport). The sample was placed in a holder locked onto a motorized micrometer stage (M-431, Newport) driven by a PC. This enabled an accurate determination of the sample position as it was translated in 0.5 μm steps through the focal point of the laser beam.

The optical beam was mechanically chopped (model 220A, HMS). A signal photodiode (PD2) detected the transmitted light as the sample was translated through the focal point of the laser beam whilst a reference photodiode (PD1) was used to monitor any long time intensity fluctuations of the laser, that were subsequently corrected for in the acquired signal. The transmitted beam was attenuated prior to the detector with neutral density filters (NDC-25C-2, Thor labs) to ensure a linear response of the detector over the entire incident power range investigated. Both signals were fed to lock-in amplifiers (signal: EG&G model 186A, Princeton Applied Research, reference: EG&G model 5206 Princeton Applied Research) referenced to the frequency (140 Hz) of the chopper and recorded on a PC through an analogue to digital board (AX5214, 48 bit DIO board, Axiom Technology Co. Ltd.). A Z-scan of the solvent blank was performed to confirm no two-photon absorption, optical breakdown or boiling of the solvent[31] was occurring over the entire excitation power range as well as to account for any background signals due to irregularities on the faces of the cuvette. Experimental investigations were conducted at pulse energies within the range of 0–880 nJ.

A 2 mm pathlength quartz cell was used in order to satisfy the prerequisites for using the "thin sample" approximation, where the sample length is small enough that changes in the beam diameter arising from diffraction or nonlinear refraction may be neglected.[27] All glassware was thoroughly acid washed prior to use. Fresh samples were made up to a concentration in the range of 10^{-3}–10^{-4} M immediately prior to measurements.

Analysis of the Z-scan data was performed as described elsewhere[26] using the Solver program in Microsoft Excel®. A 10 mM Rhodamine 6G (Rh6G) in methanol sample was used as a reference compound (see discussion below) to obtain experimental parameters such as the pulse width and beam focussing characteristics. These parameters were then kept constant in the subsequent analysis of the porphyrins. The characteristics of the laser beam needed for the analysis of the results were calculated using formulae presented elsewhere.[32] The residuals value, being the difference between the experimental and the fitted value at each position, is obtained and the Solver program set to vary the value of the two-photon absorption coefficient term as the sum of the square of the residuals over all the scanned positions converges to a minimum value.

Two-photon induced fluorescence experiments

The TPIF emission experiments used essentially the same experimental set-up described above, however, a shorter pulse laser source was employed. The Ti:sapphire oscillator (Coherent MIRA Seed), operating at 76 MHz with pulse duration of approximately 50 fs substituted the older MIRA oscillator. The pulses were stretched temporally prior to seeding the REGA 9050 operating at 250 kHz pulse repetition rate with energy of ~4 μJ per pulse. The pulses were then compressed, to compensate for the stretching that had occurred previously and also to offset any dispersion that occurred in the amplifier and transport optics, to approximately the original width of 50 fs with an average power of 2 W. The pulse–pulse stability of the laser was monitored by a fast photodiode and the pulse train displayed on an oscilloscope.

A similar experimental set-up as used in the Z-scan experiment was used to monitor the two-photon induced fluorescence intensity. The silicon photodiodes were substituted with a high sensitivity photomultiplier (Farnell Instruments) and placed adjacent to the sample perpendicular to the excitation path. A

monochromator (Jobin-Yvon H10) placed in front of the detector allowed spectral resolution of the fluorescence signal. The sample in a 1 cm pathlength cuvette was positioned at the focal point and the detected fluorescence signal at the set wavelength on the monochromator was fed to a lock-in amplifier and the intensities recorded manually.

The average excitation power was varied in the same manner as in the Z-scan experiment. Acquisition of a quadratic relationship between peak excitation power and fluorescence intensity confirms the fluorescence response is due to a two-photon excitation event.[33] The energies per pulse used for these experiments ranged from 0–400 nJ.

The fluorescence intensities are used to obtain a two-photon absorption cross-section for the photosensitiser using eqn (1)

$$\sigma_{2s} = \frac{c_r}{c_s}\frac{I_{\lambda_s}}{I_{\lambda_r}}\frac{\mathrm{FI}_{\lambda_s}}{\mathrm{FI}_{\lambda_r}}\frac{\sum \mathrm{FI}_r}{\sum \mathrm{FI}_s}\frac{\Phi_r}{\Phi_s}\sigma_{2s} \quad (1)$$

where the subscripts r and s designate the reference and the sample respectively. The term σ_2 is the two-photon absorption cross section, c is the concentration, I_λ is the two-photon induced fluorescence intensity at the wavelength λ, FI_λ is the one-photon induced fluorescence at wavelength λ and $\sum$FI is the integrated intensity of the one-photon induced fluorescence spectra. Φ represents the one-photon fluorescence quantum yield, which is assumed to be the same under two-photon excitation conditions. The two-photon induced emission signal was monitored at 625 nm for the free-base forms and 590 nm for the metallated form of the porphyrins. Concentrations used for the TPIF cross-section measurements were generally two to three orders of magnitude lower (*i.e.* in the μM range) compared with the Z-scan measurements.

It should be noted that while, in theory, the Z-scan method can provide absolute values for σ_2, both methods used here rely on the use of an assumed value for the σ_2 of a reference compound; Rh6G in methanol in the present case. There is, however, discrepancy in the reported σ_2 values of Rh6G in methanol, which therefore influences the magnitudes of the σ_2 reported here. A range of reported values of σ_2 for this dye at ~800 nm are summarised in Table 1, which indicates the uncertainty in the value that can be adopted. We have chosen to use the value for the σ_2 of the reference compound to be 16.2 GM reported by Sengupta *et al.*[36] since it is reasonably conservative in magnitude and was achieved by a method that should return absolute values. It is worth noting, however, that the concentrations used in the current study were significantly lower than the concentrations used in the cited paper (especially in the case of the TPIF measurements). We determined the σ_2 values of some well-known fluorophores that can be readily excited by two-photon absorption; Fluorescein, Rhodamine B and Rose Bengal. These values were in excellent agreement with those determined elsewhere for these compounds using an excitation wavelength of 800 nm when the appropriate correction is made for the relative magnitudes of the reference compound is taken into account.

Two-photon time resolved fluorescence microscopy

C6 rat glioma cells were obtained from the American Type Culture Collection (http://www.attcc.org). A single cell suspension harvested in the logarithmic growth phase was seeded onto microscope coverslips and grown in 2 mL of RPMI-1640 medium supplemented with a 10% fetal calf serum (FCS) both obtained from the Commonwealth Serum Laboratories (CSL, Parkville, Australia). Cells were grown to 40% confluence at 37 °C at which point an aliquot of BOPP solution (3.0 mg ml^{-1} in 0.9% saline) of the appropriate volume was added to the culture to yield the final concentration. Four independent cultures were prepared, beginning with a control culture (*i.e.* no BOPP), and an additional three cultures having final BOPP concentrations of 10, 30 and 50 μg mL^{-1}, respectively. In each case, the flasks were then re-incubated at 37 °C for a further 24 h. Immediately before imaging, the medium was removed and the adherent cells were washed twice with RPMI-1640 medium containing 10% FCS to remove exogenous BOPP, and cells were suspended in 10 mL of phosphate-buffered saline (PBS) in a custom volumetric imaging mount ensuring cell viability throughout the imaging session.

A Ti:Sapphire mode-locked laser cavity (Coherent, Mira 900F) pumped by a 10 W Nd:Vanadate laser (Coherent, Verdi V10) was used as the illumination source. This laser produces ultrashort optical pulses with a temporal pulse width of approximately 100 fs (~3 nJ pulse energy) at a repetition rate of 76 MHz. The laser beam was coupled to an inverted microscope (Olympus, IX71) through a confocal scanning unit (Olympus, FV-300) and a transfer lens, which produces a focused scanning spot moving across the normal focal plane of an imaging objective. The average excitation power at the sample was approximately 15 mW. Each image was obtained over a scan time of 90 s. A dichromatic mirror (UV-Cold Mirror, TFI Inc.) mounted at 45° in the rotating filter turret of the microscope efficiently allows incident illumination to pass up to fill the back aperture of an imaging objective, (Olympus, 40 × 1.4 NA, oil) while reflecting the emitted visible fluorescence from the sample to a PMT detector (PMC-100-1, Becker & Hickl, Germany) masked with a blocking filter (BG39, TFI Inc.).

Table 1 A selection of the reported two-photon absorption cross-sections of Rhodamine 6G in methanol using ultrashort laser pulses at ~800 nm

σ_2/GM	Method	Conc.	Laser pulse rep. rate	Laser pulse energy	Ref.
~30	TPIF	110 μM	82 MHz	~nJ	34
243.5	TPIF	10^{-5}–10^{-3}	82 MHz	~nJ	35
16.2	NLT	10.23 mM	10 Hz	0.6 mJ	36
134	TPIF	0.326 μM	100 Hz[b]	10 nJ–200 μJ	28
12.8	NLT	0.233 mM	Single pulse[b]	10 nJ–200 μJ	28
6.4 (2.9)[a] 4.2 (2.8)[a]	Fluor. saturation	1 μM	250 kHz	~nJ	37

[a] Indicates σ_2^{sat}. [b] Picosecond pulses used.

Time-resolved two-photon fluorescence images were obtained using a complete electronic system for recording fast light signals by time-correlated single photon counting (SPC-830, Becker & Hickl, Germany). The SPC-830 is a compact solution that combines all the components necessary for TCSPC measurements onto a single PCI board. Synchronised data collection is achieved with the SPC-830 board using the *x* and *y* laser scanning signals generated by the microscope scanner. Laser pulses are detected by a high-speed PIN photodiode mounted inside the mode-locking cavity of the laser and are used by the SPC-830 board to determine the detection time of a photon (anode pulse from the PMT) relative to the laser pulses. The so-called "reversed TAC mode"[38] is employed whereby the timing process is initiated by the laser synchronised signal and stopped by the detection of a fluorescence photon. This mode exploits the high pulse repetition rate of the laser source and allows for higher photon count rates. The temporal evolution of the emission probability after excitation is described by a histogram of these time spans whereby each counting event is allocated to a temporal bin for each pixel of the image. For analysis, a separate off-line software package (SPCImage, Becker & Hickl) applies a Levenberg–Marquardt routine for nonlinear fitting to fit a decay curve to the data of the model function given in eqn (2), which assumes that the fluorescence decay histogram for each pixel is well described by a multi-exponential decay.

$$I(t) = \sum_{i=0}^{n} a_i \exp^{(-t/\tau_i)} + c. \quad (2)$$

Results and discussion

The near centrosymmetric nature of the porphyrins investigated in the current study suggests that the parity selection rules for TPA are applied.[39] Therefore, in order to observe a large σ_2 requires a transition to *g*-parity excited states. Quantum mechanical calculations on porphyrin type molecules have determined that such states could be populated through two photon excitation of high energy transitions close to the Soret band.[40] Interestingly, such wavelengths also correspond to those found within the so called "biological transparency window" enabling a higher depth of penetration into biological tissue. Therefore, an excitation wavelength of 800 nm was chosen in the current two-photon investigation.

We have determined the σ_2 values obtained for the free-base and di-cation forms (classified by solvent acid) of the porphyrins in the various solvents measured by the open aperture Z-scan and TPIF methods. The various merits of the nonlinear transmission (NLT *e.g.* Z-scan), and TPIF methods and some reasons for the controversy stemming from the discrepancies produced have been discussed elsewhere.[28] Other issues such as the sample concentration that can be studied effectively and the pulse width, repetition rate and energy of the laser source, may also play a role. The sample concentration may impact through light scattering (due to solubility problems) or molecular aggregation phenomena. The pulse width should be minimised to reduce any impact of excited state transient absorption when nanosecond duration pulses are used, and pulse energies should also be minimised to avoid a range of potential nonlinearities and higher order effects. Pulse repetition rate may influence the measurements through thermal considerations.

The results of the Z-scan and TPIF measurements under a range of conditions are compared in Table 2. In general the σ_2 of the porphyrins monitored by two techniques are in excellent agreement, despite the difference of several orders of magnitude in porphyrin concentration used in the two sets of measurements (μM for TPIF and mM for the Z-scan measurements). No significant difference in the calculated σ_2 is observed for the various forms of the porphyrins in the different solvents. It should be noted that the definition of σ_2 describes the efficiency of a sample molecule to absorb two photons of light simultaneously. HpD is known to consist of a mixture of oligomers and dimers, making an accurate determination of the molecular weight problematic. Therefore, an averaged molecular weight value is used in these calculations (598.7 g mol^{-1}) as used in a previous study.[41]

Determination of σ_2 for the BOPP di-cation was unable to be obtained using the TPIF method due to the non-fluorescent nature of this form. This loss of fluorescence exhibited from the di-cation form of a porphyrin is unusual. It is known that the addition of two extra protons to the core leads to an overcrowding of the macrocycle. In order to relieve the steric strain induced, the planarity of the ring is lost. Although one should expect such crowding to be observed from the other two porphyrins investigated in the current study, it is though that the bulky nature of the *closo*-carborane substituents of BOPP serves to augment the non-planar nature of the ring. Non-planar porphyrins are known to exhibit very low fluorescence quantum yields. The values of σ_2

Table 2 Comparison of the two-photon absorption cross-sections (GM) of the porphyrins studied using the Z-scan (~10^{-3} M) and TPIF (~10^{-6} M) measurements under a range of conditions. A value for the σ_2 of Rh6G in methanol of 16.2 GM was used in each case. TPIF measurements were performed in methanol

	Z-scan						
Sample	MeOH	EtOH	Acetone	MeOH acid	EtOH acid	Acetone acid	TPIF
HPp9	11	14	9	8	8	13	9.2
Hp9-Zn							13.6
Hp9 di-cation							11.8
HpD	12	10	15	15	13	16	10.7
HpD-Zn							17.5
HpD di-cation							16.1
BOPP	10	15	14	7	13	12	9.4
BOPP-Zn							10.9
BOPP di-cation							—

for the dilute samples of the porphyrins determined by TPIF are presented in Table 2. A similar trend is observed for the different forms of each of the three porphyrins. Although the largest σ_2 is observed for the Zn porphyrins in each case, the difference in σ_2 for the various forms is small.

Most tetrapyrroles are thought to exhibit a σ_2 of at least 10 GM.[42,43] The values obtained in the current study using the open aperture Z-scan experiment are in general agreement with this estimate. They are also in reasonable agreement with the value of 7.4 ± 2.2 GM at 850 nm reported very recently for Photofrin determined at a concentration of ~100 μg mL^{-1}.[44] Assuming a molar mass of Photofrin of 596.8 g mol^{-1},[45] this corresponds to a concentration of ~1.7 × 10^{-4} M which is approximately two orders of magnitude higher than the concentration used here for the TPIF measurements.

In order to determine the suitability of the porphyrins characterised in this study for PDT, we performed two-photon imaging studies on rat C6 glioma cells transfected with the free-base form of BOPP of various concentrations and control cells (*i.e.* no porphyrin present). Although the two-photon absorption cross-sections for this series of porphyrins reported herein are low (which is in agreement with other work[44]) the cross-section is sufficient for two-photon fluorescence imaging purposes. This is illustrated in Fig. 3(a), 3(b) and 3(c), which depict time-resolved two-photon images, collected over 90 second acquisition periods, of cells with BOPP concentrations of 10, 30 and 50 μg mL^{-1}, respectively. The control cells did exhibit some very weak background (auto-) fluorescence, however, this was only detectable after an accumulated image acquisition time of 5 min. The emission is shown to be due to two-photon absorption by the nonlinear dependence of the emission intensity on incident excitation power, which has a gradient of approximately 2.0 as expected for a two-photon absorption event (Fig. 4).

Previous investigations using a rather simple implementation of time-resolved, single photon confocal fluorescence imaging[46,47] have shown BOPP to localise primarily to the mitochondria within C6 glioma cells with very little evidence of BOPP associated with membranes, the nucleus, cytoplasm or exogenously.[48] The time-resolved, two-photon fluorescence images of BOPP-loaded C6 glioma cells, recorded as a function of loading concentration indicate that the emission from BOPP largely originates from within the perinuclear region of the cell, but that at the concentrations used, which are higher than the previous investigations,[46–48] the uptake of BOPP is a little more widely distributed than previously reported. It is also clear that there are distinct changes in the fluorescence lifetime throughout the cell at particular spatial locations for a given concentration. The fluorescence lifetime distributions required for use in the image analysis range between approximately 0.5 and 3.0 ns, with little indication of the long-lived free-base form. There are readily identifiable differences in the lifetime at the nuclear membrane and in the cytoplasm. At 30 μg mL^{-1} (Fig. 3(b)), the majority of the BOPP emission in the cytoplasm appears to originate from the di-cation form (τ_f ~ 2 ns[46,47]) with some evidence of the mono-cation form (τ_f ~ 0.8 ns[46,47]) in the nuclear membrane region. We also see some evidence of BOPP emission (from a short-lived form) from within the nucleus, which has not been reported previously. This emission becomes identifiable in the time-resolved fluorescence images whereas it may not be evident in conventional (steady-state) fluorescence images since the former do not represent the intensity of the emission (related to concentration, absorption coefficient, fluorescence quantum yield and collection efficiency), but rather identify the presence of emitting species on the basis of their fluorescence lifetime. It should be pointed out that the significant shortening of the fluorescence lifetime distribution to less than 1.0 ns in Fig. 3(c) is likely due to the fact that the cell is clearly stressed and dying due to the increased concentration of the porphyrin. The clarity of the images compared with those from the earlier study using single-photon excitation imaging methods

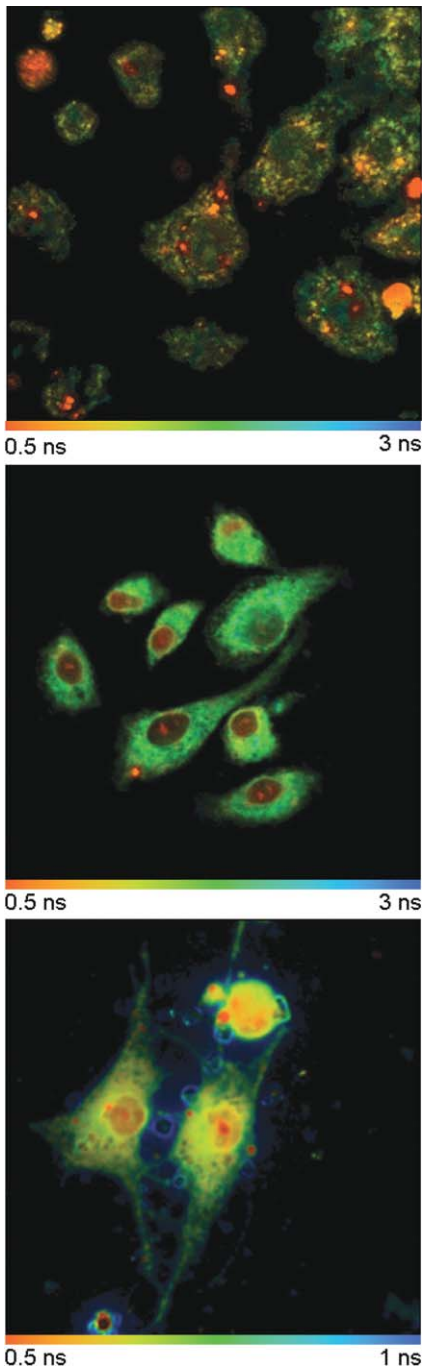

Fig. 3 Time-resolved two-photon fluorescence images of BOPP in C6 glioma cells with loading of (a) 20, (b) 30 and (c) 50 μg mL^{-1}.

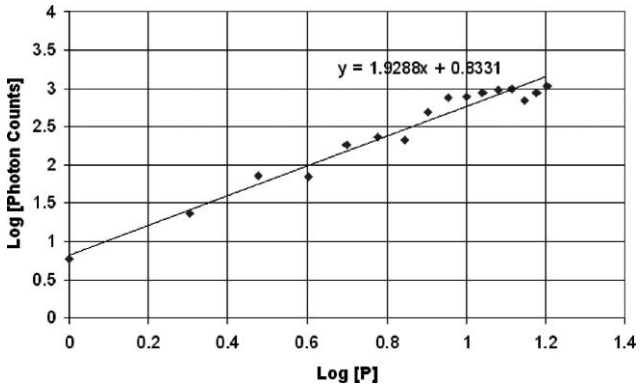

Fig. 4 Log–log plot of fluorescence intensity from BOPP-loaded C6 Glioma cells indicating a slope of ~2 illustrating that emission is due to two-photon-induced absorption.

is noticeably enhanced using a two-photon method of excitation. The ability to assign emitting species with particular fluorescence lifetimes associated with specific regions of the cell provides further insight into intracellular distribution and speciation over steady-state measurements.

Conclusions

The two-photon absorption cross-sections of a series of porphyrin photosensitisers have been determined under a range of conditions, and by both Z-scan and TPIF methods. Although the porphyrins studied here exhibit low two-photon cross-sections of ~10 GM and low fluorescence quantum yields compared to the reference compounds used, with the advancements made in detection devices, they are shown (by using BOPP as an example) to be adequate fluorophores for use in two-photon microscopy applications. Through our imaging studies we have shown that a porphyrin concentration level of ~30 μg mL^{-1} is the optimum level to provide the highest possible signal to noise ratio while maintaining cell viability. Time-resolved, two-photon fluorescence imaging has been used to identify the forms of BOPP present in particular regions of the cell, highlighting the advantage of such measurements over conventional, steady-state imaging methods.

Abbreviations

BOPP, tetrakiscarborane carboxylate ester of 2,4-(α,β-dihydroxyethyl)deuteroporphyrin IX; Hp9, hematoporphyrin IX dihydrochloride; HpD, hematoporphyrin derivative; TPIF, two-photon induced fluorescence; TPA, two-photon absorption; NLT, nonlinear transmission method *e.g.* Z-scan.

Acknowledgements

This work has been supported in part by the Australian Research Council and the Victorian Institute for Chemical Sciences.

Notes and references

1 C. N. Ironside, *Contem. Phys.*, 1993, **34**, 1.
2 T. Sekikawa, T. Kanai and S. Watanabe, *Phys. Rev. Lett.*, 2003, **91**, 103902.
3 O. Lammel and A. Penzkofer, *Opt. Quant. Electr*, 2000, **32**, 1147.
4 G. Zhou, X. Wang, D. Wang, Z. Shao and M. Jiang, *Appl. Opt.*, 2002, **41**, 1120.
5 M. G. Silly, L. Porrès, O. Mongin, P.-A. Chollet and M. Blanchard-Desce, *Chem. Phys. Lett.*, 2003, **379**, 74.
6 T. Yu, C. K. Ober, S. M. Kuebler, W. Zhou, S. R. Marder and J. W. Perry, *Adv. Mater.*, 2003, **15**, 517.
7 S. Maruo, K. Ikuta and H. Korogi, *Appl. Phys. Lett.*, 2003, **82**, 133.
8 H. E. Pudavar, M. P. Joshi, P. N. Prasad and B. A. Reinhardt, *Appl. Phys. Lett.*, 1999, **74**, 1338.
9 R. W. Boyd, *Nonlinear Optics*, Academic Press, New York, 1993.
10 R. L. Swofford and A. C. Albrecht, *Ann. Rev. Phys. Chem.*, 1978, **29**, 421.
11 J. D. Bhawalkar, G. S. He and P. N. Prasad, *Rep. Prog. Phys.*, 1996, **59**, 1041.
12 D. W. Piston, *Trends Cell Biol.*, 1999, **9**, 66.
13 W. G. Fischer, W. P. Partridge, C. Dees and E. A. Wachter, *Photochem. Photobiol.*, 1997, **66**, 141.
14 J. M. Song, T. Inoue, H. Kawazumi and T. Ogawa, *Anal. Sci.*, 1999, **15**, 601.
15 P. Schwille, U. Haupts, S. Maiti and W. W. Webb, *Biophys. J.*, 1999, **77**, 2251.
16 V. E. Centonze and J. G. White, *Biophys. J.*, 1998, **75**, 2015.
17 W. Denk, J. H. Strickler and W. W. Webb, *Science*, 1990, **248**, 73.
18 G. J. Brakenhoff, M. Muller and R. I. Ghauharali, *J. Microsc.*, 1996, **183**, 140.
19 Y. Mir, D. Houde and J. E. Van Lier, *Photochem. Photobiol. Sci.*, 2006, **5**, 1024.
20 R. L. Goyan and D. T. Cramb, *Photochem. Photobiol.*, 2000, **72**, 821.
21 J. Liu, Y. W. Zhao, J. Q. Zhao, A. D. Xia, L. J. Jiang, S. Wu, L. Ma, Y. Q. Dong and Y. H. Gu, *J. Photochem. Photobiol., B*, 2002, **68**, 156.
22 D. Gao, R. R. Agayan, H. Xu, M. A. Philbert and R. Kopelman, *Nano Lett.*, 2006, **6**, 2383.
23 K. Kandasamy, S. J. Shetty, P. N. Puntambekar, T. S. Srivastava, T. Kundu and B. P. Singh, *J. Porphyrins Phthalocyanines*, 1999, **3**, 81.
24 I. E. Borissevitch, A. G. Bezzeerra-Jr, A. S. L. Gomes, R. E. De Araujo, C. B. De Araujo, K. M. T. Oliveira and M. Trsic, *J. Porphyrins Phthalocyanines*, 2001, **5**, 51.
25 B. P. Singh, R. Vijaya, T. Kundu, K. Kandasamy, P. N. Puntambekar, S. J. Shetty and T. S. Srivastava, *J. Porphyrins Phthalocyanines*, 2001, **5**, 439.
26 E. W. Van Stryland and M. Sheik-Bahae, Z-scan measurements of optical nonlinearities, in *Characterization Techniques and Tabulations for Organic Nonlinear Materials*, ed. M. G. Kuzyk and C. W. Dirk, Marcel Dekker, Inc, 1998, p. 655.
27 M. Shiek-Bahae, A. A. Said, T.-H. Wei, D. J. Hagan and E. W. Van Stryland, *IEEE J. Quantum Electron.*, 1990, **QE-26**, 760.
28 D. A. Oulianov, I. V. Tomov, A. S. Dvornikov and P. M. Rentzepis, *Opt. Commun.*, 2001, **191**, 235.
29 S. B. Kahl and M.-S. Koo, *J. Chem. Soc., Chem. Commun.*, 1990, **24**, 1769.
30 M. Gouterman, G. H. Wagniere and L. C. Snyder, *J. Mol. Spectrosc.*, 1963, **11**, 108.
31 A. Gnoli, L. Razzari and M. Righini, *Opt. Express*, 2005, **13**, 7976.
32 S. Venugopal Rao, D. Narayana Rao, J. A. Akkara, B. S. DeCristofana and D. V. G. L. N. Rao, *Chem. Phys. Lett.*, 1998, **297**, 491.
33 M. Göppert-Mayer, *Ann. Phys.*, 1931, **9**, 273.
34 P. Sengupta, J. Balaji, S. Banerjee, R. Philip, G. Ravindra Kumar and S. Maiti, *J. Chem. Phys.*, 2000, **112**, 9201.
35 M. A. Albota, C. Xu and W. W. Webb, *Appl. Opt.*, 1998, **37**, 7352.
36 A. Fischer, C. Cremer and E. H. K. Stelzer, *Appl. Opt.*, 1995, **34**, 1989.
37 M. Kauert, P. C. Stoller, M. Frenz and J. Ricka, *Opt. Exp.*, 2006, **14**, 8434.
38 D. V. O'Connor and D. Phillips, *Time-Correlated Single Photon Counting*, Academic Press, London, 1984.
39 M. McClain, *Acc. Chem. Res.*, 1974, **7**, 129.
40 X.-J. Liu, J.-K. Feng, A.-M. Ren and X. Zhou, *Chem. Phys. Lett.*, 2003, **373**, 197.
41 P. Murasecco, E. Oliveros, A. M. Braun and P. Monnier, *Photobiochem. Photobiophys.*, 1985, **9**, 193.
42 M. Drobizhev, A. Karotki, K. Kruk and A. Rebane, *Chem. Phys. Lett.*, 2002, **355**, 175.

43 A. Karotki, M. Kruk, M. Drobizhev and A. Rebane, *J. Mod. Opt.*, 2002, **49**, 379.
44 A. Karotki, M. Khurana, J. R. Lepock and B. C. Wilson, *Photochem. Photobiol.*, 2006, **82**, 443.
45 A. Holder and D. Lagostera, 2004, http://lagrange.math.trinity.edu/tumath/research/reports/report88.pdf.
46 P. G. Spizzirri, J. S. Hill, S. B. Kahl and K. P. Ghiggino, *Photochem. Photobiol.*, 1996, **64**, 975.
47 P. G. Spizzirri, J. S. Hill, S. B. Kahl and K. P. Ghiggino, *Lasers Med. Sci.*, 1996, **11**, 237.
48 J. S. Hill, S. B. Kahl, A. H. Kaye, S. S. Stylli, M.-S. Koo and M. F. Gonzales, *Proc. Natl. Acad. Sci. USA*, 1992, **89**, 1785.

